A fused polycyclic compound containing phenothiazine and diazapyrene skeletons with weak D–A interactions

Keito Matsumoto, Yoshimitsu Tachi, Masatoshi Kozaki

Matsumoto, K., Tachi, Y., & Kozaki, M. (2022). A fused polycyclic compound containing phenothiazine and diazapyrene skeletons with weak D–A interactions. *Chemical Communications*. 58, 8572–8575. https://doi.org/10.1039/d2cc02635j

COMMUNICATION

Fused Polycyclic Compound Containing Phenothiazine and Diazapyrene Skeletons with Weak D-A interactions

Keito Matsumoto, Yoshimitsu Tachi and Masatoshi Kozaki*

Received 00th January 20xx,
Accepted 00th January 20xx

DOI: 10.1039/x0xx00000x

A small fused polycyclic molecule containing a phenothiazine and diazapyrene skeleton as the donor and acceptor, respectively, has a redox potential similar to those of the corresponding donor and acceptor molecules, indicating that the inherent electronic properties of the donor and acceptor were retained due to weak orbital interactions.

Phenothiazines (PTZs) are considered excellent electron-rich building blocks for the construction of electronic,[1] optical,[2] and magnetic materials.[3] Recently, a variety of PTZ-based extended fused-ring systems have been produced by condensing electron-rich rings to enhance their electron-donating ability (**A**–**C**, Fig. 1).[4] There are a few donor (D)-acceptor (A)-type fused-ring compounds with a PTZ framework and electron-deficient conjugating rings.[5] In sharp contrast, PTZ units are often connected to A-units with single bonds or conjugated bridges to obtain advanced functional materials, such as photo-emitters with thermally activated delayed emission or photo-induced charge-separating systems.[6]

For some applications, weak intramolecular D–A interactions, and spatial separation of the HOMO and LUMO are essential for obtaining the desired function of the D–A type molecule.[7] D–A-type fused-ring systems with flat structures facilitate strong intermolecular π–π interactions. The proximity of the electron-rich and electron-poor rings, however, usually induces strong D–A interactions in the ground state, resulting in the attenuation of electron donating and accepting abilities and large HOMO–LUMO energy gaps.[8] Recently, Hatakeyama et al. achieved an efficient HOMO–LUMO separation with multiple resonance effects.[9] Their research revealed that small D–A type fused-ring systems with weak HOMO–LUMO interaction can be produced by suitably conjugated topologies. However, small polycyclic fused compounds with weak intramolecular D–A interactions are limited, and a conjugation topology suitable for reducing the D–A interactions has not yet been established.

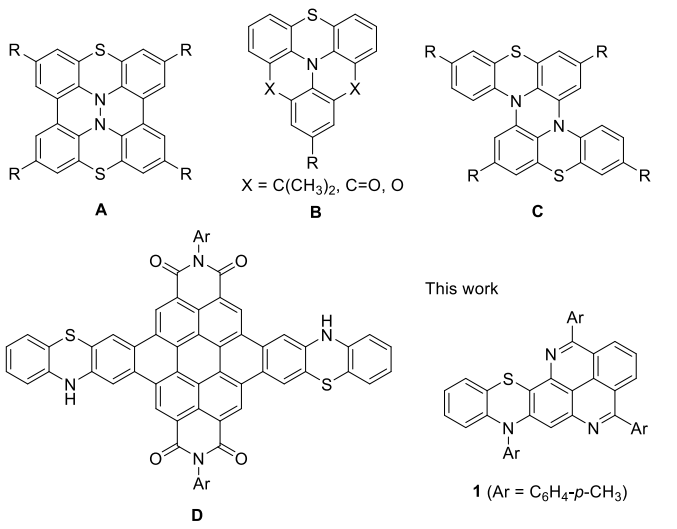

Fig. 1. Representative phenothiazine-based fused-ring compounds and this work.

Herein, we report the compact fused-ring system **1** with PTZ and diazapyrene (DAP) units joined by one benzene ring as the donor and acceptor, respectively. In previous studies, extension of the conjugation was often achieved using an aromatic ring at a nitrogen atom in the PTZ unit (Fig.1).[4] This is a rare example of π-extension of the PTZ unit with an aromatic ring connected at the 3-position, followed by double annulation at the 2- and 4-positions. The structure and properties of **1** were investigated by means of X-ray structural analyses, spectral and electrochemical measurements, and theoretical calculations, and the results indicate that the inherent electron-donating and electron-accepting abilities of the PTZ and DAP skeletons, respectively, are unexpectedly retained in the fused-ring system due to the unique conjugation topology.

Graduate School of Science, Osaka City University 3-3-138, Sugimoto, Sumiyoshi-ku, Osaka 558-8585, Japan

†Electronic Supplementary Information (ESI) available: [Synthetic procedures, NMR spectra, cetacean coordinate of optimized structures.]. See DOI: 10.1039/x0xx00000x

Scheme 1. Synthesis of **1**.

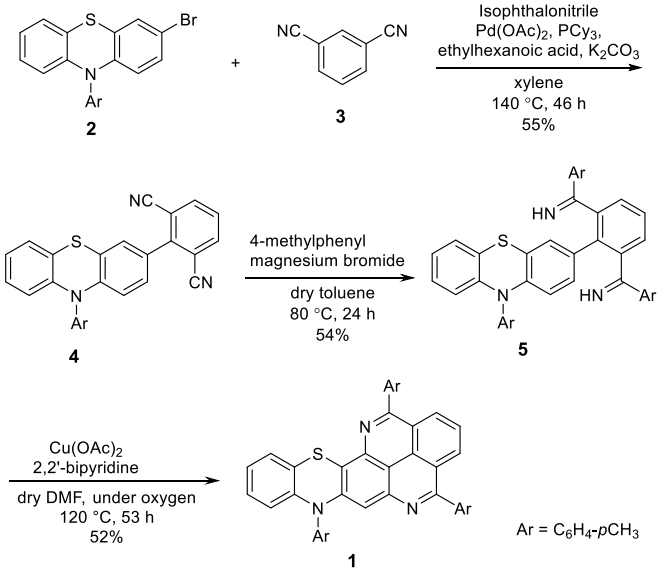

Compound **1** was synthesized from 3-bromo-10-(4-methylphenyl)-10*H*-PTZ (**2**) using a previously reported double-annulation protocol (Scheme 1).[10] Compound **2** was prepared in two steps from the easily accessible 10*H*-phenothiazine using a previously reported method.[11] Direct C–H arylation of isophthalonitrile (**3**) with **2** was carried out using palladium acetate, tri(cyclohexyl)phosphine (Cy_3P), potassium carbonate, and 2-ethylhexanolic acid to produce **4** in 55% yield.[12] The nucleophilic addition of 4-methylphenylmagnesium bromide to **4** followed by treatment with methanol, formed bisimine **5** in 54% yield.[13] Compound **1** was obtained as a purple solid in 52% yield by copper-catalyzed oxidative double transannular cyclization of **1**.[10,13] PTZ was successfully converted to **1** in only five steps. The structure of **1** was characterized in a detailed manner using NMR spectroscopy, MS analysis, and X-ray structural analysis.

A single crystal of **1** suitable for X-ray structural analysis was obtained as a black plate by slow vapor diffusion of diethyl ether into a dichloromethane solution of **1** (Fig. 2 and Table S1). Although neutral PTZ units typically have a butterfly structure in the solid state[14], the fused-ring framework of **1** unpredictably has an almost planar structure with a slight bend. The dihedral angle (φ) between the benzene rings in the PTZ unit in **1** is 170 °, which is significantly larger than that in 10-phenyl-10*H*-phenothiazine (**6**, φ = 153 °, Fig. 3).[15] Neutral PTZ skeletons with relatively planar conformations were reported for some PTZ-based D–A type molecules, such as **C** (φ = 175 °).[5,16] The C–S (1.763(2) and 1.756(2) Å) and C–N (1.408(3) and 1.420(2) Å) bond lengths in ring *B* are typical of the neutral PTZ unit.[14,15] The C–N (imine) bonds *e* (1.386(2) Å) and *f* (1.386(2) Å) are similar in length to the closely related DAP derivative (1.40 Å).[17] In the crystal, **1** formed a slipped-stacking structure in a head-to-head and tail-to-tail fashion (Fig. S1) that involved intermolecular C–C contacts (3.32 and 3.38 Å), slightly shorter than the sum of the van der Waals radii (3.40 Å). The substituted tolyl groups in the DAP unit had large dihedral angles with the adjacent rings *D* and *E* (43.0° and 42.3°).

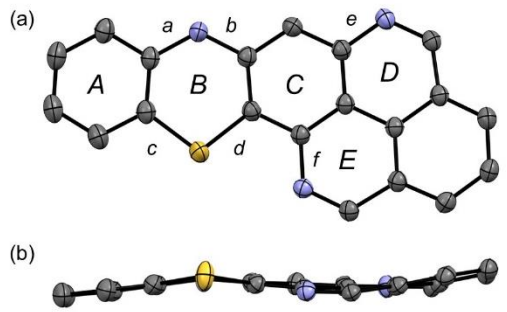

Fig. 2. ORTEP diagrams of **1**: (a) Top view, (b) Side view (Blue, yellow, grey, and white shows nitrogen, sulfur, and carbon atoms, respectively. 4-Methyl phenyl groups and hydrogen atoms were omitted for clarity. Italic symbols denote assigned names of the selected bonds and ring positions.

The UV-Vis spectrum of **1** was measured at room temperature in dichloromethane (ε = 8.9, 4.53 × 10^{-5} M) and compared with those of 10-(4-methylphenyl)-10*H*-phenothiazine (**7**) and 5,9-di(4-methylphenyl)-4,10-diazapyrene (**8**) to gain insight into the electronic structure in the ground state (Fig. 4). Compound **1** produced a characteristic broad absorption band in the visible region, with maximum absorption (λ^{abs}_{max}) at 522 nm. Absorption band for **7** and **8** were observed in the shorter-wavelength region up to 400 nm. Time-dependent density functional theory (DFT) calculations at the CAM-B3LYP/6-31+g(d,p) level of theory were performed to assign the absorption band of **1** in the visible region (λ^{calcd}_{max} = 451 nm, f = 0.1625), indicating that the HOMO–LUMO transition is the dominant contributor to this electronic transition. As described below, the DFT calculation results suggested that the HOMO and LUMO are found predominantly on the PTZ and DAP units, respectively. Therefore, the HOMO–LUMO band was characterized by short-range intramolecular charge transfer (ICT). The optical HOMO–LUMO energy gap (E_g^{opt}) was estimated to be 2.00 eV from the terminal wavelength of long-wavelength absorption (619 nm). The absorption spectra of **1** were recorded in toluene (ε = 2.4, 3.07 × 10^{-5} M) and DMF (36.7, 3.29 × 10^{-5} M) (Fig. S2). The λ^{abs}_{max} of the ICT band was slightly blue-shifted by 11 nm upon increasing the solvent polarity (λ^{abs}_{max} = 516 (toluene,) and 527 (DMF)), indicating that **1** has a small dipole moment in the ground state. These results suggest the presence of a weak interaction between the PTZ and DAP units in the ground state. The calculated dipole moment (2.51 D) further supported the weakly polar character of **1** in the ground state.

To determine the electronic structure in the excited state, the fluorescence spectrum of **1** was measured at room temperature (Fig. S3). Considerable red shifts were observed for

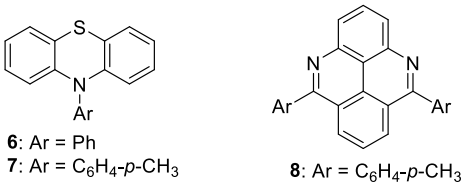

Fig. 3. Chemical structures of reference compounds.

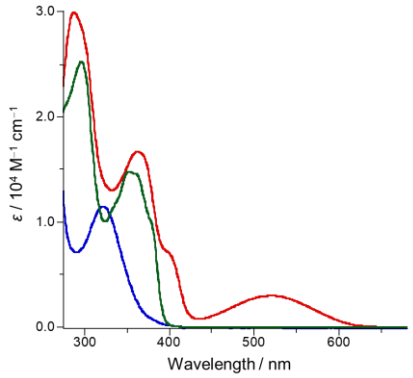

Fig. 4. UV-Vis spectra of **1** (red line, 4.53 × 10^{-5} M), **7** (blue line), and **8** (green line) in dichloromethane.

the fluorescence band of **1** when the solvent polarity was increased. Fluorescence maxima (λ^{em}_{max}) were observed at 620, 636, and 648 nm in toluene (λ^{ex} = 526 nm, Φ_f = 0.26), dichloromethane (green line, λ^{ex} = 522 nm, Φ_f = 0.091), and DMF (blue line, λ^{ex} = 526 nm, Φ_f = 0.058), respectively. Therefore, the Stokes shift increased with increasing the solvent polarity (3250 cm^{-1} (toluene), 3430 (dichloromethane), and 3540 (DMF)). These results indicate that **1** has a larger dipole moment in the excited state than in the ground state.[18]

Cyclic voltammograms of **1** were measured in benzonitrile using tetrabutylammonium perchlorate (nBu$_4$NClO$_4$), a Pt disk electrode, and Pt wire as the supporting electrolyte, working electrode, and counter electrode, respectively, at a scan rate of 100 mV/s. Reversible oxidation and reduction waves were observed at half-wave potentials ($E^{1/2}$) of +0.35 and −1.88 V vs Fc/Fc^+, respectively (Fig. 5). The oxidation potential of **1** was comparable to that of **7** ($E^{1/2}_{ox}$ = +0.37 V vs Fc/Fc^+),[19] indicating that the electron-donating ability of the PTZ unit was maintained in the fused-ring system of **1**. The HOMO energy level of **1** was estimated to be −5.15 eV from the oxidation potential. However, the reduction potential of **1** cathodically shifted 0.25 V compared to that of **8** ($E^{1/2}_{red}$ = −2.13 V vs Fc/Fc^+),[19] suggesting that the inherent electron-accepting ability of the DAP unit was retained in the fused-ring system in **1**. The LUMO energy level of **1** was calculated to be −2.92 eV using the reduction potentials. The electrochemical HOMO–LUMO

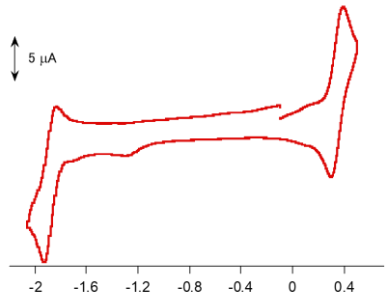

Fig. 5. Cyclic voltgammogram of **1** in benzonitrile (nBu$_4$NClO$_4$, a Pt disk electrode, and Pt wire as a supporting electrolyte, working electrode, and counter electrode, respectively, at a scan rate of 100 mV/s.).

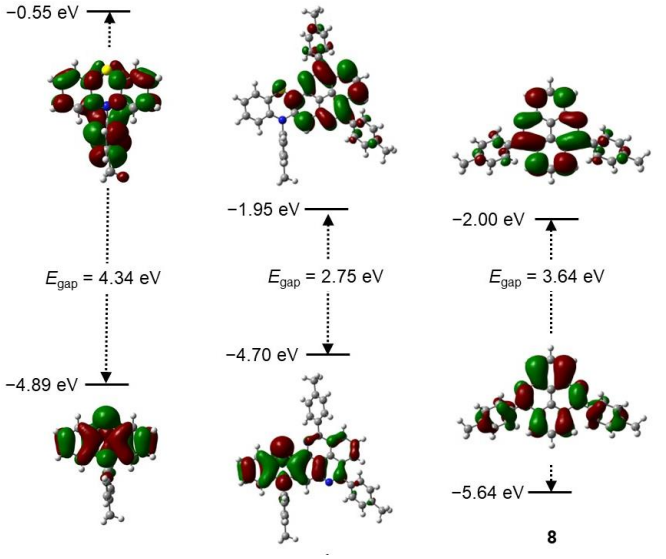

Fig. 6. Energy diagrams of the Kohn–Sham HOMOs and LUMOs of **1**, **7**, and **8** obtained from DFT calculations (B3LYP/6-31G(d,p)).

energy gap (E_g^{ec}) was determined to be 2.23 eV, which was consistent with E_g^{opt} (2.00 eV).

To determine the detailed features of the frontier orbitals, DFT calculations were performed at the B3LYP/6-31G(d,p) level of theory for **1** and **7**. The results were compared with those reported for **8** (Fig. 6). The HOMO energy level of **1** was calculated to be −4.70 eV, which is comparable to that of **7** (−4.89 eV), indicating that the PTZ units in **1** maintain their inherent electron donating ability. The LUMO energy level of **1** was estimated to be −1.95 eV, which is very similar to that of **8** (−2.00 eV), suggesting that **1** has an electron-accepting ability comparable to that of **8**. The HOMO and LUMO of **1** are predominantly localized on the PTZ and DAP units, respectively. The distinct orbital shapes of the HOMO of **7** and the LUMO of **8** are reminiscent of the HOMO and LUMO of **1**, respectively. These results suggest the presence of weak intramolecular interactions between the PTZ and DAP units in **1**. The narrow HOMO–LUMO gap (2.75 eV) was evaluated for **1** because the HOMO and LUMO energy levels of **1** are almost the same as those of **7** and **8**, respectively. This value is slightly larger than the experimentally obtained values (E_g^{opt}: 2.00 eV, E_g^{ec}: 2.23 eV).

The aromaticities of **1** and **6** were evaluated by calculating nucleus-independent chemical shifts (NICS) using the GAO-CAM-B3LYP/6-31G+(d,p) level of theory (Fig. 7 and Table S4). The initial geometries were extracted from the respective crystal structures. The NICS(0) value for hetero six-membered ring *B* of **1** were +8.43, which are considerably higher than those

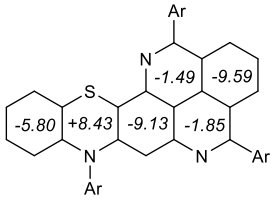

1

Fig. 7. NICS(0) values of **1** (GAO-CAMB3LYP/6-31G+(d,p)).

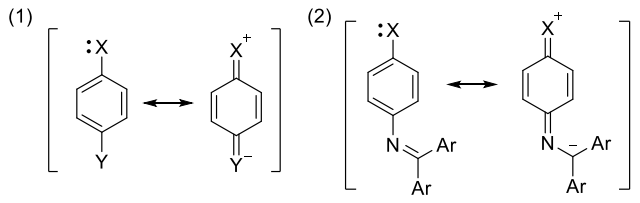

Fig. 8. Conjugation topologies with (1) strong and (2) weak D-A interactions (X: electron rich atoms, and Y: electron poor atoms).

of **6** (+4.43). These results indicate that the structural change from a butterfly to planar structure enhances the antiaromaticity of ring *B*. The inner benzene ring *C* in **1** has a small NICS(0) (−9.13), which indicates that ring *C* possesses high aromaticity. This was further supported by the large harmonic oscillator model of aromaticity values (0.95) of ring *C*. This consideration is consistent with the absence of a stable quinoidal resonance structure for ring *C*. The weak intramolecular D–A interaction was attributed to the lack of a stable zwitterionic resonance structure of the conjugated system in **1** (Fig. 8). Bridging a nitrogen atom in a diarylimine group and an electron-donating heteroatom (X in Fig. 8) with phenylene linker is probably useful approach to reduce D–A interactions.

In conclusion, a compact D–A type fused-ring compound was synthesized with PTZ and DAP units as the donors and acceptors, respectively. The PTZ and DAP units in the fused-ring system maintained their inherent electronic donating and accepting abilities, respectively, owing to their unique conjugated topology. Through this research, novel strategy for designing a small D–A type fused-ring system with negligible intramolecular D–A interactions was proposed. Another combination of electron donating and accepting frameworks with the similar π-topology is desired to study the scope and limitation of the proposed strategy. Research on compounds with similar conjugation topologies and their applications is currently in progress.

This work was supported by JSPS KAKENHI (Grant numbers: JP17K05790, and JP20K05466). There are no conflicts to declare.

Notes and references

1 K. Kozawa, T. Hoshizaki, and T. Uchida, *Bull. Chem. Soc. Jpn.*, 1991, **64**, 2039; H. Kobayashi, *Bull. Chem. Soc. Jpn.*, 1973, **46**, 2945.
2 Z. Zhou, C. E. Hauke, B. Song, X. Li, P. J. Stang, and T. R. Cook, *J. Am. Chem. Soc.*, 2019, **141**, 3717; J. A. Christensen, B. T. Phelan, S. Chaudhuri, A. Acharya, V. S. Batista, and M. R. Wasielewski, *J. Am. Chem. Soc.,* 2018, **140**, 5290; S. Suzuki, D. Yamaguchi, Y. Uchida, and T. Naota, *Angew. Chem. Int. Ed.*, 2021, **60**, 8284.
3 T. Tahara, S. Suzuki, M. Kozaki, D. Shiomi, K. Sugisaki, K. Sato, T. Takui, Y. Miyake, Y. Hosokoshi, H. Nojiri, and K. Okada, *Chem. Eur. J.*, 2019, **25**, 7201.
4 S.-i. Kato, T. Matsuoka, S. Suzuki, M. S. Asano, T. Yoshihara, S. Tobita, T. Matsumoto, and C. Kitamura, *Org. Lett.*, 2020, **22**, 734; Yokoyama, N. Tanaka, N. Fujimoto, R. Tanaka, S. Suzuki, D. Shiomi, K. Sato, T. Takui, M. Kozaki, and K. Okada, *Chem. Asian J.*, 2021, **16**, 72; D. Sakamaki, D. Kumano, E. Yashima, and S. Seki, *Chem. Commun.*, 2015, **51**, 17237.
5 M. Kojima, A. Tamoto, N. Aratani, and H. Yamada, *Chem. Commun.*, 2017, **53**, 5698.
6 R. Y. Lai, X. Kong, S. A. Jenekhe, and A. J. Bard, *J. Am. Chem. Soc.*, 2003, **125**, 12631; H. Tanaka, K. Shizu, H. Nakanotani, and C. Adachi, *J. Phys. Chem. C*, 2014, **118**, 15985.
7 H. Uoyama, K. Goushi, K. Shizu, H. Nomura, and C. Adachi, *Nature,* 2012, **492**, 234.
8 Y.-J. Cheng, Y.-J. Ho, C.-H. Chen, W.-S. Kao, C.-E. Wu, S.-L. Hsu, and C.-S. Hsu, *Macromolecules*, 2012, **45**, 2690; C. Jia, S.-X. Liu, C. Tanner, C. Leiggener, A. Neels, L. Sanguinet, E. Levillain, S. Leutwyler, A. Hauser, and S. Decurtins, *Chem. Eur. J.,* 2007, **13**, 3804.
9 T. Hatakeyama, K. Shiren, K. Nakajima, S. Nomura, S. Nakatsuka, K. Kinoshita, J. Ni, Y. Ono, and T. Ikuta, *Adv. Mater.,* 2016, **28**, 2777.
10 Y. Omura, Y. Tachi, K. Okada, and M. Kozaki, *J. Org. Chem.*, 2019, **84**, 2032.
11 S1. S.-H. Park, O-H. Kwon, W.-J. Paek, U.S. Patent US20090026928 A1 2009-01-29; T. Okamoto, M. Kozaki, M. Doe, M. Uchida, G. Wang, K. Okada, *Chem. Mater.*, 2005, **17**, 5504; Y. Liang, P. Yuyu, T. Xiangyang, B. Qing, S. Fangzhong, L. Feng, L. Ping, Y. Bing M. Yuguang, *J. Phys. Chem. C*, 2015, **119**, 17800.
12 N. E. Ihanainen, E. T. T. Kumpulainen, A. M. P. Koskinen, *Eur. J. Org. Chem.,* 2015, **2015**, 3226.
13 S. Chiba, *Bull. Chem. Soc. Jpn.,* 2013, **86**, 1400; L. Zhang, G. Y. Ang, S. Chiba, *Org. Lett.,* 2010, **12**, 3682.
14 T. Okamoto, M. Kuratsu, M. Kozaki, D. Shiomi, K. Sato, T. Takui, and K. Okada, *Org. Lett.*, 2004, **6**, 3493.
15 Y. Wang, J. Yang, M. Fang, Y. Gong, J. Ren, L. Tu, B. Z. Tang, and Z. Li, *Adv. Funct. Mat.*, 2021, **31**, 2101719.
16 T. Zhang, Y. Han, J. Huo, and P. Xue, *CrystEngComm*, 2020, **22**, 5137.
17 Y. Han, Z. Hu, M. Liu, M. Li, T. Wang, and Y. Chen, *J. Org. Chem.*, 2019, **84**, 3953.
18 J. R. Lakowicz, Principles of Fluorescence Spectroscopy, Springer, Berlin, 3rd edn, 2006.
19 Redox potentials of **7** and **8** were measured under identical conditions.

